JOURNAL OF VIROLOGY, Mar. 2007, p. 2792–2804 Vol. 81, No. 6
0022-538X/07/$08.00+0 doi:10.1128/JVI.01760-06

Oncolytic Vesicular Stomatitis Virus Induces Apoptosis via Signaling through PKR, Fas, and Daxx[▽]

Daniel F. Gaddy† and Douglas S. Lyles*

Department of Biochemistry, Wake Forest University School of Medicine, Winston-Salem, North Carolina 27157

Received 14 August 2006/Accepted 18 December 2006

Matrix (M) protein mutants of vesicular stomatitis virus (VSV) are promising oncolytic agents for cancer therapy. Previous research has implicated Fas and PKR in apoptosis induced by other viruses. Here, we show that dominant-negative mutants of Fas and PKR inhibit M protein mutant virus-induced apoptosis. Most previous research has focused on the adapter protein FADD as a necessary transducer of Fas-mediated apoptosis. However, the expression of dominant-negative FADD had little effect on the induction of apoptosis by M protein mutant VSV. Instead, virus-induced apoptosis was inhibited by the expression of a dominant-negative mutant of the adapter protein Daxx. These data indicate that Daxx is more important than FADD for apoptosis induced by M protein mutant VSV. These results show that PKR- and Fas-mediated signaling play important roles in cell death during M protein mutant VSV infection and that Daxx has novel functions in the host response to virus infection by mediating virus-induced apoptosis.

During the process of tumorigenesis, many cancers develop defects in their antiviral responses (25). This is due to the principle that proliferative signaling pathways and antiviral signaling pathways are often mutually antagonistic (5, 7, 9, 58, 59). Therefore, the development of enhanced proliferative signaling in cancer cells may lead to the suppression of antiviral pathways, which are also antiproliferative. For example, it has been shown that many cancer cells are resistant to the antiproliferative effects of interferons (IFNs) due to defects in the IFN signal transduction pathway of these tumors (25, 68). This resistance of cancer cells to the effects of IFN makes these cells correspondingly more susceptible to infection with a variety of viruses, including vesicular stomatitis virus (VSV) (1, 5, 7, 58).

VSV is a well-studied prototype for the large group of negative-strand RNA viruses. It is one of the most rapidly cytocidal viruses due to the potent induction of apoptosis in infected cells. The susceptibility or resistance of different tissues to VSV is determined by a variety of factors. For example, it has been shown that defective control of translation is a feature of tumorigenesis that can facilitate VSV replication (4). Susceptibility to VSV is also regulated by the ability to mount an IFN response (46, 49), allowing VSV to selectively infect cancer cells with defects in their IFN responses but not normal cells with intact IFN responses. The selectivity of VSV for such cancers can be enhanced by mutating viral proteins that suppress host IFN responses (1, 59) or by incorporating genes that enhance antiviral responses such as interleukin-4 or IFN (27, 51).

The oncolytic potential of VSV against a variety of cancers has been established (1, 5, 7, 22, 23, 35, 45, 58, 59, 67). Recent research in this area has focused on identifying mechanisms to enhance this oncolytic potential or to enhance the selectivity of these viruses for cancer cells as opposed to normal cells (1, 17, 24, 51, 56, 59). One such strategy involves the use of matrix (M) protein mutants of VSV to enhance tumor selectivity. This strategy is based on work from our laboratory and others showing that the M protein is the major viral suppressor of host gene expression (46). M protein mutant viruses that are defective in their ability to inhibit host gene expression induce the expression of IFNs and other antiviral gene products, while viruses containing wild-type (WT) M protein suppress host antiviral responses (1, 59). As a result, viruses with WT M protein can infect susceptible normal tissues, such as the central nervous system, as well as susceptible cancers, while M protein mutant viruses can infect susceptible cancers but not normal tissues such as the central nervous system (1, 59). In in vivo models of cancer, M protein mutant virus is as effective as virus with WT M protein at eliminating tumors with defective interferon responses, while neither virus is effective at eliminating tumors with intact interferon responses (1).

An important aspect of these endeavors is to understand the mechanism by which VSV mutants induce oncolysis. We have previously demonstrated that M protein mutant VSV induces apoptosis via a pathway that is distinct from that activated by WT VSV (29). In particular, M protein mutant VSV primarily activates the upstream caspase, caspase-8 (29), while viruses with WT M protein primarily activate caspase-9 (8, 41). Furthermore, apoptosis induced by M protein mutant viruses involves the induction of new host gene expression, while apoptosis induced by viruses with WT M protein is due to the inhibition of host gene expression (29, 41). The purpose of the work presented here was to determine the mechanism of cell death induced by an M protein mutant VSV that is a promising candidate for oncolytic virus therapy. Since a major component of host antiviral responses is the induction of apoptosis requiring the upregulation of proapoptotic genes and their products, we hypothesize that apoptosis induced by VSV M protein mutants is due to the induction of host antiviral responses. If

* Corresponding author. Mailing address: Department of Biochemistry, Wake Forest University School of Medicine, Winston-Salem, NC 27157. Phone: (336) 716-4237. Fax: (336) 716-7671. E-mail: dlyles@wfubmc.edu.

† Present address: Department of Molecular Genetics and Biochemistry, University of Pittsburgh School of Medicine, Pittsburgh, PA 15261.

▽ Published ahead of print on 27 December 2006.

so, the induction of apoptosis should involve a program of proapoptotic gene expression and should be activated through known mediators of apoptosis in response to virus infection, such as Fas/CD95 and the antiviral protein kinase PKR (6, 8, 16, 28, 50, 60). Here, we show that M protein mutant VSV induces the expression of a program of proapoptotic genes, while these genes are suppressed during infection with WT VSV. Furthermore, we show that apoptosis induced by M protein mutant VSV was inhibited by the expression of dominant-negative mutants of Fas and PKR. While most previous research has focused on the cytoplasmic adapter protein FADD as a necessary transducer of Fas-mediated signaling, our data show that an alternative adapter protein, Daxx, is more important than FADD for the induction of apoptosis by rM51R-M virus. While Daxx has previously been implicated in antiviral responses to some DNA viruses and retroviruses (13, 33, 34, 62, 74), this is the first description of a requirement for Daxx in virus-induced apoptosis. These data provide important new insights into the induction of apoptosis by viruses as well as further elucidate the mechanism of cytolysis induced by a promising agent for oncolytic viral therapy.

MATERIALS AND METHODS

Viruses, plasmids, and cells. L929 mouse fibroblasts were cultured in Dulbecco's modified Eagle medium (DMEM) supplemented with 7% fetal bovine serum. The recombinant viruses rWT and rM51R-M were obtained from cDNA clones and grown as previously described (42). Virus titers were determined by plaque assay on BHK cells. Experiments shown were conducted under single-cycle growth conditions in which L929 cells were infected at a multiplicity of infection of 20 PFU per cell to ensure synchronous infection. Similar results were obtained under multiple-cycle growth conditions (multiplicity of infection of 0.1 PFU per cell), although the induction of apoptosis was slower than that under single-cycle virus growth (data not shown).

The dominant-negative Fas (ΔFas) was generated from L929 cell RNA using reverse transcription-PCR (RT-PCR). The primers used were sense primer 5′-GCGAATTCATGCTGTGGATCTGG, containing a 5′ EcoRI site, and antisense primer 5′-GCCTCGAGCTACTCAGCTGTGTCTTGGATGC, containing a 5′ XhoI site (72). The RT-PCR product was cut with EcoRI and XhoI and ligated into plasmid pcDNA3.1-Puro(+) containing a puromycin resistance gene (a gift of Andrew Thorburn, University of Colorado Health Sciences Center). Stable L929-ΔFas cells were generated by transfecting L929 cells with plasmid pcDNA3.1-puro(+)-ΔFas as previously described (41). Simultaneously, L929-empty vector (EV) cells were generated by transfecting L929 cells with plasmid pcDNA3.1-puro(+). Stably transfected cells were selected in DMEM supplemented with 10% fetal bovine serum and 1 μg/ml puromycin.

Plasmid pEYFP-ΔFADD was a gift from Andrew Thorburn. The ΔFADD gene was digested from plasmid pEYFP using XhoI and ApaI and ligated into plasmid pcDNA3.1-Puro(+). Stable L929-ΔFADD cells were generated by transfecting L929 cells with the pcDNA3.1-puro(+)-ΔFADD plasmid as described above.

Dominant-negative Daxx (ΔDaxx) was generated from L929 cell RNA using RT-PCR. The primers used were sense primer 5′-GCGAATTCGAAATGAGC AAGAGATTT CGG, containing a 5′ EcoRI site, and antisense primer 5′-GC CTCGAGCTAATCAGAGTCTG AAAGCACG, containing a 5′ XhoI site (54). The RT-PCR product was cut with EcoRI and XhoI and ligated into plasmid pcDNA3.1-puro(+). Stable L929-ΔDaxx cells were generated by transfecting L929 cells with plasmid pcDNA3.1-puro(+)-ΔDaxx as described above.

Plasmid pETFVA$^-$-PKR$_{K296P}$ expressing dominant-negative PKR was obtained from Randall Kaufman. Dominant-negative PKR contains the lysine-to-proline substitution at position 296 (K296P), rendering the dominant-negative PKR molecule defective in its kinase activity but fully functional in its ability to bind double-stranded RNA (dsRNA) (69). The dominant-negative PKR gene was digested from plasmid pETFVA$^-$ with KpnI and BamHI and ligated into plasmid pcDNA3.1-puro(+). Stable L929-ΔPKR cells were generated by transfecting L929 cells with pcDNA3.1-puro(+)-ΔPKR as described above.

Microarrays. L929 cells were mock infected or infected with either rWT or rM51R-M virus. At 16 h postinfection, total RNA was isolated using TRIzol reagent (Invitrogen). Fifteen micrograms of each RNA sample was processed according to the manufacturer's protocol (Affymetrix) and hybridized to the Affymetrix MOE 430A gene chip. The MOE 430A chip provides coverage of more than 14,000 characterized mouse genes. Each chip was scaled to a target intensity of 5,000, normalized to the 100 control probe sets present on each chip, and then expressed as a ratio to mock-infected samples or the nonspecific background on a per-gene basis. Analysis of microarray data was carried out using Affymetrix Data Mining Tool software (Affymetrix).

Western blot analysis. L929 cells were grown to about 75% confluence in 6-well dishes and were infected with recombinant viruses. At the indicated times postinfection, cells were solubilized in radioimmunoprecipitation assay buffer containing 1 mM phenylmethylsulfonyl fluoride, 1 mM aprotinin, 1 mM pepstatin, 100 nM okadaic acid, and 100 nM microcystin. Proteins were resolved by sodium dodecyl sulfate-polyacrylamide gel electrophoresis on 10% polyacrylamide gels. Following electrophoresis, gels were electroblotted onto polyvinylidene difluoride and blocked in Tris-buffered saline (pH 7.5) containing 5% bovine serum albumin. Immunoblots were then probed with antibodies against Fas or Daxx (Santa Cruz) or promyelocytic leukemia (PML) protein (Upstate). Protein band intensities were quantitated by scanning and analysis with Quantity One software (Bio-Rad).

Flow cytometry. All flow cytometry experiments were carried out using a FACSCaliber instrument (BD Biosciences). Apoptosis induction was measured by incubating cells with annexin V (BD Pharmingen) and 7-amino actinomycin D (7-AAD; BD Pharmingen) at room temperature for 15 min and acquiring samples immediately. Fas surface expression was measured by incubating cells with phycoerythrin (PE)-conjugated anti-Fas antibodies (Cell Signaling) for 30 min on ice. Background fluorescence was detected in these experiments with a PE-conjugated mouse immunoglobulin G2a isotype control antibody (Cell Signaling). Active caspase-3 was detected by staining cells intracellularly with PE-conjugated anti-active caspase-3 antibodies using a CytoFix/CytoPerm kit according to the manufacturer's instructions (BD Pharmingen). PKR activation was measured by staining cells intracellularly with primary antibodies that recognize phospho-PKR (Thr446; Cell Signaling). Jun N-terminal kinase (JNK) activation was measured by staining cells intracellularly with primary antibodies that recognize total JNK (Cell Signaling) and phospho-JNK (Thr183 and Tyr185; Cell Signaling) and secondary anti-rabbit antibodies conjugated to Alexa-488 (Invitrogen). Data were analyzed using CellQuest Pro software (BD Immunocytometry Systems).

Inhibition of FasL, PKR, and JNK activities. To inhibit FasL signaling, 30 μg/ml of FasL neutralizing antibody (Nok1; BD Pharmingen) (38) was added to cells at the time of infection with rM51R-M virus. As a positive control for the activity of Nok1 antibody, 10 μg/ml of recombinant FasL (rFasL; Calbiochem) and 30 μg/ml of Nok1 were preincubated in DMEM at 37°C for 1 h before addition to cells in the presence of cycloheximide to enhance Fas signaling as described previously (73). Where indicated, cells were pretreated for 30 min with 20 mM 2-aminopurine (Sigma) to inhibit PKR activity or 25 μM SP600125 (Calbiochem) to inhibit JNK activity.

Time-lapse microscopy. Cells were grown to about 50% confluence in 6-well dishes and infected with recombinant viruses. Infected cells were incubated for 30 min at room temperature while rocking to allow the attachment of virus to cells. Cells were then transferred to an environmental chamber attached to a Zeiss Axiovert S200 microscope. Time-lapse microscopy was also used to quantitate the rate of apoptosis induced by tumor necrosis factor (TNF)-related apoptosis-inducing ligand (TRAIL) (50 ng/ml; R&D Systems). Images were captured at 15-min intervals using a Hamamatsu charge-coupled-device camera run by Openlab software (Improvision) and were saved in QuickTime movie format. Cells were monitored for 48 h to detect cells entering apoptosis, as determined by the appearance of membrane blebbing.

Caspase-8 activity assays. L929 cells were grown to about 50% confluence in 24-well dishes. Cells were infected with the recombinant viruses or treated with TRAIL as indicated in the figure legends. Each experiment was performed in duplicate. Caspase activity was determined with a fluorogenic substrate for caspase-8 (IETD-AFC; R&D Systems) according to the protocol provided by the manufacturer. Each sample was incubated for 2 h with the peptide substrate, and fluorescence intensities were measured at excitation and emission wavelengths of 400 nm and 505 nm, respectively, using a Safire II fluorescent microplate reader (Tecan). Bradford assays (Bio-Rad) were conducted to measure total protein concentrations.

Indirect immunofluorescence. Cells to be stained for immunofluorescence were grown on coverslips. Indirect immunofluorescence assays were conducted as previously described (52). Briefly, monolayers were fixed with 4% paraformaldehyde for 10 min at room temperature and then permeabilized with 0.2% Triton X-100 for 5 min at room temperature and washed three times with

Tris-buffered saline plus 5 mg/ml bovine serum albumin, 1 mg/ml glycine, and 0.05% Tween-20 (TBS-BGT). Primary antibodies were incubated with the cells for 1 h at room temperature in TBS-BGT and then washed four times with TBS-BGT. Secondary antibodies were incubated with the cells for 30 min at room temperature in TBS-BGT, and cells were washed four times with TBS-BGT. Nuclear DNA was stained with 4′,6′-diamidino-2-phenylindole (DAPI). Coverslips were mounted onto glass slides using Aqua-Mount (Lerner Laboratories). In all cases, control experiments showed no cross-reactions between the fluorophores, and images obtained by staining with individual antibodies were the same as those obtained by double labeling. Images were acquired as 8-bit TIFF files with a Nikon Eclipse TE300 inverted microscope equipped with a monochrome Retiga EX 1350 digital camera (QImaging Corp.), a 60× 1.4-numerical-aperture oil immersion objective, and a 1.4-numerical-aperture differential interference contrast oil immersion condenser lens. Micrographs were generated from the TIFF images using Photoshop 7.0 (Adobe Systems Inc.) to adjust brightness and contrast in a uniform manner. Antibodies used were rabbit anti-Daxx (Santa Cruz), mouse anti-PML (Upstate), anti-rabbit Alexa-568 (Invitrogen), and anti-mouse Alexa-488 (Invitrogen).

Statistical analysis. A paired Student's *t* test was used to compare significances of individual time points. A P value of <0.05 was considered to be statistically significant.

RESULTS

VSV infection affects the expression of genes in each major apoptotic pathway. The induction of apoptosis by M protein mutant VSV is dependent largely on the activation of the upstream caspase, caspase-8, and involves new host gene expression (29). In contrast, apoptosis induced by viruses with WT M protein is dependent primarily on the activation of caspase-9 and involves the inhibition of host gene expression by WT M protein (41). The host genes involved in the differential induction of apoptosis by virus with WT versus mutant M protein were determined by oligonucleotide microarray analysis. L929 murine fibrosarcoma cells were mock infected, infected with a recombinant wild-type VSV (rWT virus) expressing wild-type M protein, or infected with a recombinant VSV expressing the mutant M51R-M protein (rM51R-M virus). These two viruses are isogenic, with the exception of the M51R mutation in the M protein of rM51R-M virus, which renders this virus defective in its ability to inhibit host gene expression (2, 11). The expression of mRNAs for over 14,000 characterized genes was analyzed at 16 h postinfection, a time near the onset of the major apoptotic morphological changes in cells infected with rM51R-M virus (29) and when maximal expression of proapoptotic genes occurs (our unpublished data). Genes included in Fig. 1 were genes involved in the regulation of apoptosis whose signal level was significantly above the level seen with nonspecific control oligonucleotides in at least one of the experimental samples (mock-, rWT-, or rM51R-M virus-infected cells). Data shown in Fig. 1 are expressed as a ratio of the signal level in mock-infected cells, with gray indicating signals that were not significantly above nonspecific levels detected by the control (mismatched) probe set. Among genes associated primarily with death receptor pathways (Fig. 1A), a large number were expressed at higher levels in rM51R-M virus-infected cells than in mock-infected cells, although some, such as FADD and TNF receptor mRNAs, were expressed at lower levels. The most striking result was that the expression of most of these genes was suppressed below the level of detection by infection with rWT virus.

In addition to genes associated with the death receptor pathway, the expression of a number of genes associated primarily with the mitochondrial pathway (Fig. 1B) and the endoplasmic reticulum stress pathway (Fig. 1C) were induced by infection with rM51R-M virus, consistent with the observation that these pathways are also activated in infected cells, although neither of these pathways plays as large a role as the caspase-8/death receptor pathway (29). Overall, these results indicate that in-

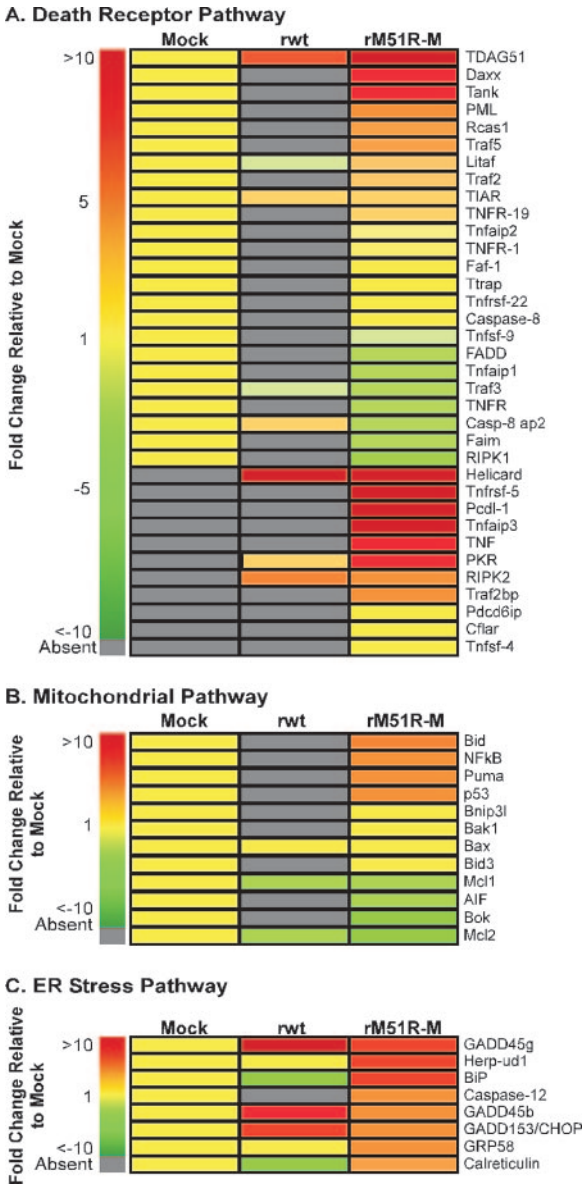

FIG. 1. rM51R-M virus infection upregulates the expression of genes associated with all three apoptotic pathways. L929 cells were mock infected or infected with rWT virus or rM51R-M virus. At 16 h postinfection, total RNA was harvested and subjected to oligonucleotide microarray analysis. Microarrays were analyzed as described in Materials and Methods. Data are expressed as a ratio of the signal level in virus-infected cells to the level in mock-infected cells and coded as induced (red), suppressed (green), or unchanged (yellow). Gray indicates signal levels that were not significantly different from the background signal of the nonspecific control probe set. (A) Genes associated with death receptor apoptotic pathways. (B) Genes associated with the mitochondrial apoptotic pathway. (C) Genes associated with endoplasmic reticulum stress-induced apoptosis. TNFR, tumor necrosis factor receptor.

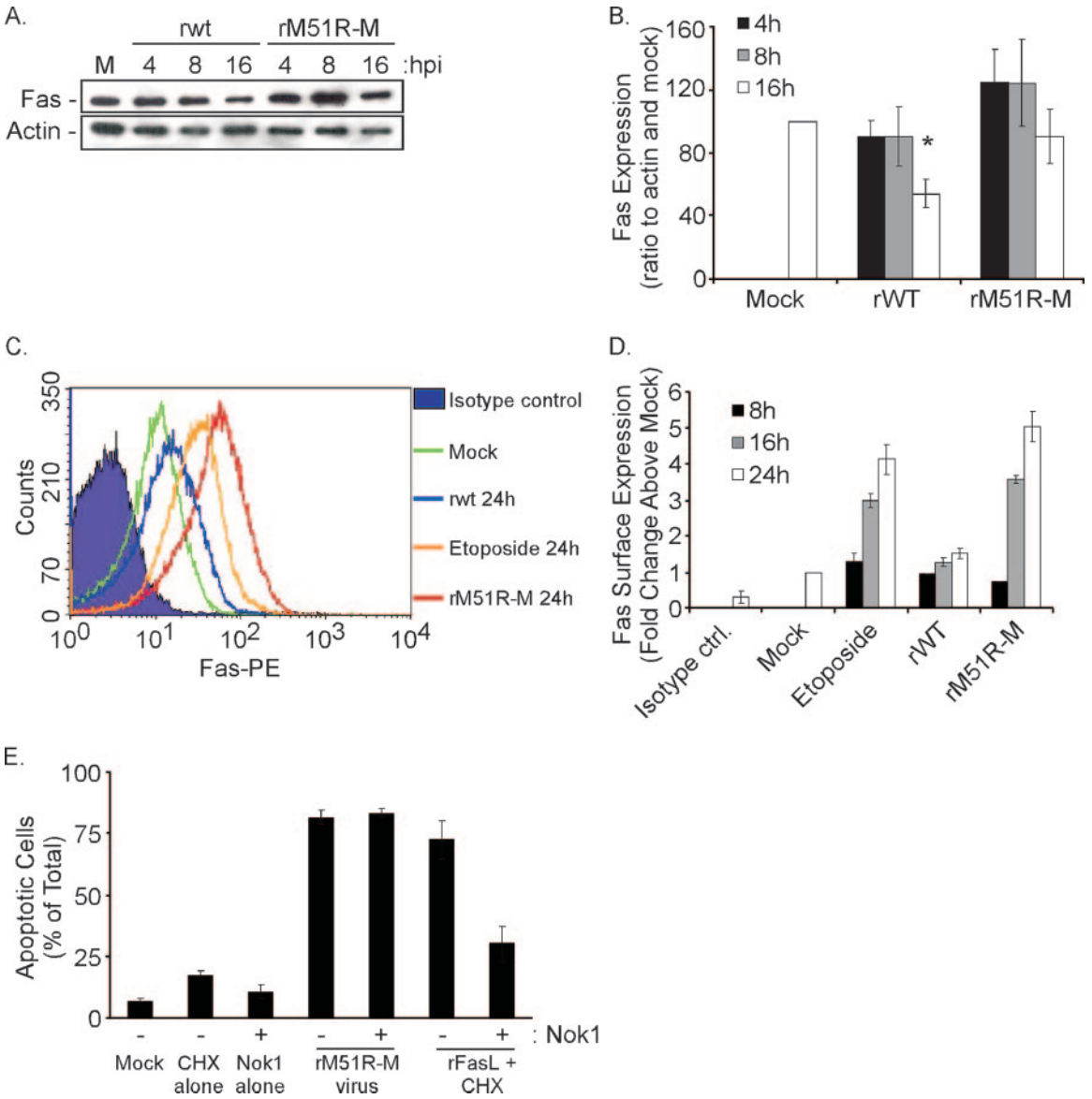

FIG. 2. rM51R-M virus infection induces the movement of the Fas death receptor to the cell surface. (A) L929 cells were mock infected or infected with rWT or rM51R-M virus. At the indicated times postinfection, cell lysates were generated and analyzed via Western blotting with antibodies for the Fas death receptor and β-actin. (B) Western blots were quantitated via densitometric analysis. Levels of Fas protein expression were normalized to levels of actin for each sample. Results represent the averages of three independent experiments ± standard errors of the means (SEM). ($*P < 0.05$ relative to mock-infected samples). (C) L929 cells were mock infected (green line), infected with rWT virus (blue line) or rM51R-M virus (red line), or treated with etoposide (orange line). At 24 h postinfection or posttreatment, levels of Fas surface expression were analyzed via flow cytometry using anti-Fas antibodies conjugated to PE. Background was determined by using a PE-conjugated mouse immunoglobulin G2 isotype control antibody. (D) Fas surface expression was analyzed at the indicated times postinfection by quantitating flow cytometry data. Data are expressed as the changes (*n*-fold) above mock-infected cells. Results are from three independent experiments ± SEM. (E) To measure the effect of blocking FasL signaling, L929 cells were untreated, infected with rM51R-M virus, or treated with rFasL and cycloheximide (CHX) in the presence or absence of FasL neutralizing antibody (Nok1). Apoptosis was measured via flow cytometry by staining with annexin V and 7-AAD. Data are presented as percentages of annexin V-positive cells and represent the average ± SEM of three experiments. hpi, hours postinfection.

fection with rM51R-M virus induces a program of gene expression that is primarily proapoptotic and that this program of gene expression is largely suppressed by infection with rWT virus.

Many of the genes that were most strongly induced during rM51R-M virus infection were genes that have been shown to play a role in the Fas death receptor pathway, although mRNA for Fas itself was not detected significantly above nonspecific hybridization in any of the samples. For experiments that follow, it is important that while mRNA expression for the adaptor protein FADD decreased during rM51R-M virus infection (Fig. 1A), the expression of mRNA for Daxx, another adaptor protein that has been implicated in Fas-mediated apoptosis (12, 71), increased almost 10-fold during rM51R-M virus in-

fection. Both FADD and Daxx mRNAs were suppressed below the level of detection during rWT virus infection. Microarray results were validated using TaqMan quantitative RT-PCR (data not shown).

Signaling through PKR and the Fas death receptor is required for rM51R-M virus-induced apoptosis. Fas-mediated signaling has been implicated in apoptosis in response to infection by a variety of viruses (10). While Fas gene expression was not detected in the microarray analysis, Fas protein was readily detected via Western blot analysis (Fig. 2A and B). Fas protein expression decreased approximately 50% from the level in mock-infected cells by 16 h postinfection with rWT virus, while Fas expression was maintained in rM51R-M virus-infected cells at levels equivalent to those of mock-infected cells.

Activation of Fas signaling is often accompanied by the translocation of Fas to the cell surface from intracellular stores (3). Surface expression of Fas protein was analyzed by immunofluorescent labeling and flow cytometry (Fig. 2C and D). L929 cells were mock infected, infected with rWT virus or rM51R-M virus, or treated with the chemotherapeutic agent etoposide as a positive control (66). Fas-specific labeling was detected on mock-infected cells at levels slightly above labeling by the nonspecific isotype control antibody, and infection with rWT virus induced only a slight increase in Fas-specific labeling. On the other hand, rM51R-M virus infection increased Fas expression on the surface of L929 cells to levels as high or higher than those on cells treated with etoposide (Fig. 2C and D). Combined with the Western blot data indicating that total Fas protein remained constant in rM51R-M virus-infected cells, the increased surface labeling indicates that Fas is transported to the cell surface from intracellular stores.

Although Fas surface expression increased in response to infection with rM51R-M virus, treatment with an antagonist Fas ligand (FasL) antibody (Nok1) to block the interaction between Fas and FasL did not inhibit rM51R-M virus-induced apoptosis (Fig. 2E). As a positive control for antibody activity, Nok1 antibody successfully inhibited apoptosis induced by treating cells with recombinant FasL in the presence of cycloheximide (Fig. 2E). Taken together, these data suggest that rM51R-M virus infection activates the Fas apoptotic pathway independent of FasL.

Several studies have indicated that the interferon-inducible dsRNA-dependent protein kinase (PKR) is involved in activating Fas- and FADD-dependent apoptosis independent of FasL. This has been observed in response to a variety of stresses, including virus infection (6, 8, 19, 20, 60). To determine whether Fas signaling and PKR signaling are involved in rM51R-M virus-induced apoptosis, L929 cells that stably express a dominant-negative Fas mutant (L929-ΔFas) and a dominant-negative PKR (L929-ΔPKR) were generated. ΔFas consists of the entire extracellular and transmembrane domains of the Fas death receptor but is truncated within the intracellular death domain, thus inhibiting interactions with adaptor proteins necessary for apoptotic signaling (72). ΔPKR contains a single point mutation converting a lysine to a proline at position 296 (K296P). This dominant-negative mutant is fully capable of binding dsRNA but is deficient in its kinase activity (69). L929-ΔFas, L929-ΔPKR, and L929 cells stably expressing an empty vector (L929-EV) were infected with rWT virus or rM51R-M virus. Cells entering apoptosis were quantitated using time-lapse microscopy and are shown in Fig. 3A and B as a function of time postinfection. The onset of membrane blebbing, an early morphological indicator of apoptosis, was used as the criterion to measure entry into apoptosis as previously described (29, 42).

As expected, both rWT and rM51R-M viruses induced apoptosis in L929-EV cells, with rM51R-M virus-infected cells entering apoptosis more rapidly than rWT virus-infected cells. While the expression of ΔFas dramatically inhibited apoptosis induced by rM51R-M virus (Fig. 3A), apoptosis induced by rWT virus was not affected by ΔFas expression (Fig. 3B). This result serves as a control for the specificity of inhibition by ΔFas, since rWT virus-induced apoptosis is not affected by the inhibition of the caspase-8/death receptor pathway (29). In contrast, the expression of ΔPKR inhibited apoptosis induction by both viruses (Fig. 3A and B). These data suggest that Fas and PKR play integral roles in apoptosis induced by rM51R-M virus, while apoptosis induced by rWT virus involves PKR but not Fas.

To confirm the results obtained by time-lapse microscopy, the activation of the initiator caspase, caspase-8, and the effector caspase, caspase-3, was analyzed at various times postinfection in L929-EV, L929-ΔFas, and L929-ΔPKR cells (Fig. 3C and D). Caspase-8 activity was measured using a fluorogenic substrate (IETD-AFC). Because this substrate has the potential to be cleaved by other caspases, the activities measured by this substrate are referred to as caspase-8-like activities. Caspase-3 activity was analyzed via flow cytometry utilizing an antibody specific for the active form of caspase-3. Cells were mock infected or infected with rM51R-M virus. For caspase-8 assays, cell lysates were analyzed at 4 h, 8 h, and 12 h postinfection. Caspase-3 activation was determined at 16 h and 24 h postinfection since the activation of caspase-3 occurs over a longer time course than does the activation of caspase-8 (29).

The maximum level of caspase-8-like activity was observed in L929-EV cells at 8 h postinfection with rM51R-M virus. In contrast, caspase-8-like activity in L929-ΔFas and L929-ΔPKR cells remained at background levels throughout this time course, confirming that ΔFas and ΔPKR act upstream of caspase-8 to inhibit apoptosis induction (Fig. 3C). Similarly, the maximum level of active caspase-3 was detected at 24 h postinfection with rM51R-M virus in L929-EV cells, while rM51R-M virus failed to activate caspase-3 above control levels in L929-ΔFas and L929-ΔPKR cells (Fig. 3D). rWT virus failed to activate caspase-8 or caspase-3 during this time course in any of these cell lines (not shown), as expected based on previously reported data (29). These data indicate that dominant-negative mutants of PKR and the Fas death receptor inhibit the induction of apoptosis by rM51R-M virus. As controls for the effectiveness of the dominant-negative mutants, the activation of PKR by phosphorylation at threonine 446 was assayed by flow cytometry using a phosphospecific antibody (Fig. 3E). Levels of phospho-PKR increased as a function of time postinfection with rM51R-M virus in untransfected L929 and L929-EV cells. In contrast, there was no increase in phospho-PKR following infection of L929-ΔFas or L929-ΔPKR cells, confirming the inhibition of signaling through this pathway.

To further test whether PKR plays a role in rM51R-M virus-

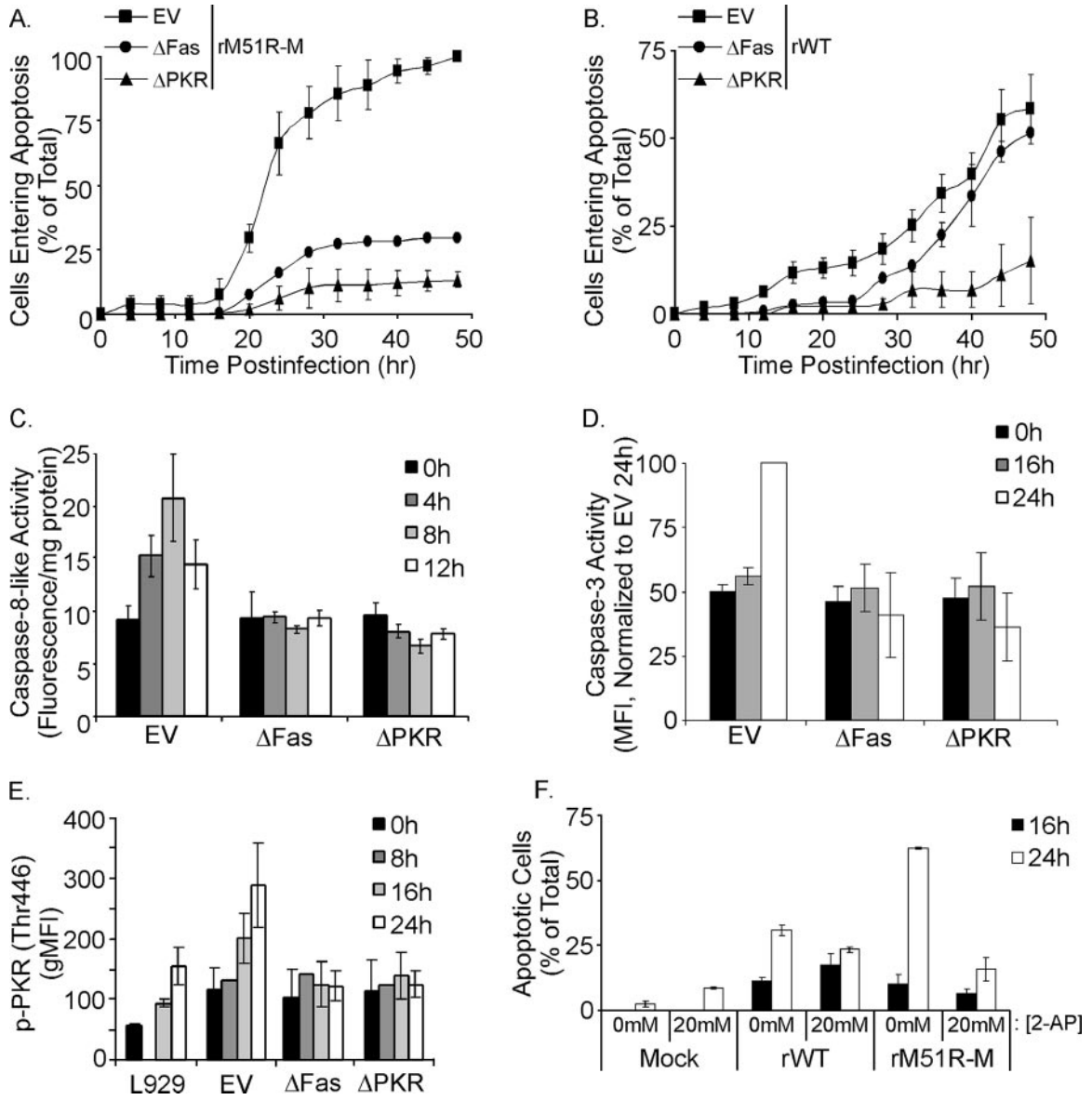

FIG. 3. Functional Fas and PKR are required for rM51R-M virus-induced apoptosis. (A) L929 cells stably expressing an empty vector control plasmid (EV) or dominant-negative mutants of Fas (ΔFas) or PKR (ΔPKR) were infected with rM51R-M virus. The cumulative percentage of cells entering apoptosis was determined using time-lapse video microscopy and is plotted as a function of time postinfection. The data represent the averages ± SEM of three experiments. (B) L929-EV, L929-ΔFas, and L929-ΔPKR cells were infected with rWT virus. Cells entering apoptosis were monitored using time-lapse video microscopy as described above (A). The data represent the averages ± SEM of three experiments. (C) Fluorometric caspase-8 assays were performed using L929-EV, L929-ΔFas, and L929-ΔPKR cells that were mock infected or infected with rM51R-M virus. At the indicated times postinfection, cells were lysed, and caspase-8 activity was measured with a fluorogenic substrate. Caspase-8 activity is expressed in arbitrary fluorescence units per mg of total protein. The data represent the average ± SEM of three experiments. (D) Caspase-3 activity was measured via flow cytometry using PE-conjugated antibodies against active caspase-3 in L929-EV, L929-ΔFas, and L929-ΔPKR cells that were mock infected or infected with rM51R-M virus. Data are expressed as the geometric mean fluorescence intensity (MFI) normalized to the maximum level observed in EV cells. The data represent averages ± SEM of three experiments. (E) Levels of PKR phosphorylation at threonine 446 were measured by flow cytometry using a phosphospecific antibody in L929, L929-EV, L929-ΔFas, and L929-ΔPKR cells that were mock infected or infected with rM51R-M virus. Data are expressed as the geometric mean fluorescence intensity (gMFI) (average of two independent experiments). (F) Apoptosis in the presence and absence of 2-AP was measured via flow cytometry by staining with annexin V and 7-AAD. Data are presented as percentages of annexin V-positive cells and represent averages ± SEM of three experiments.

induced apoptosis, L929 cells were treated with 25 mM 2-aminopurine (2-AP), an inhibitor of PKR activity, and then mock infected or infected with rWT virus or rM51R-M virus. The percentage of apoptotic cells was measured at 16 h and 24 h postinfection by labeling cells with annexin V and 7-AAD. As shown in Fig. 3F, 2-AP treatment had little effect on apoptosis induced by rWT virus during this time course. However, rM51R-M virus-induced apoptosis was reduced to near-background levels, supporting the hypothesis that PKR activity is necessary for the induction of apoptosis by rM51R-M virus

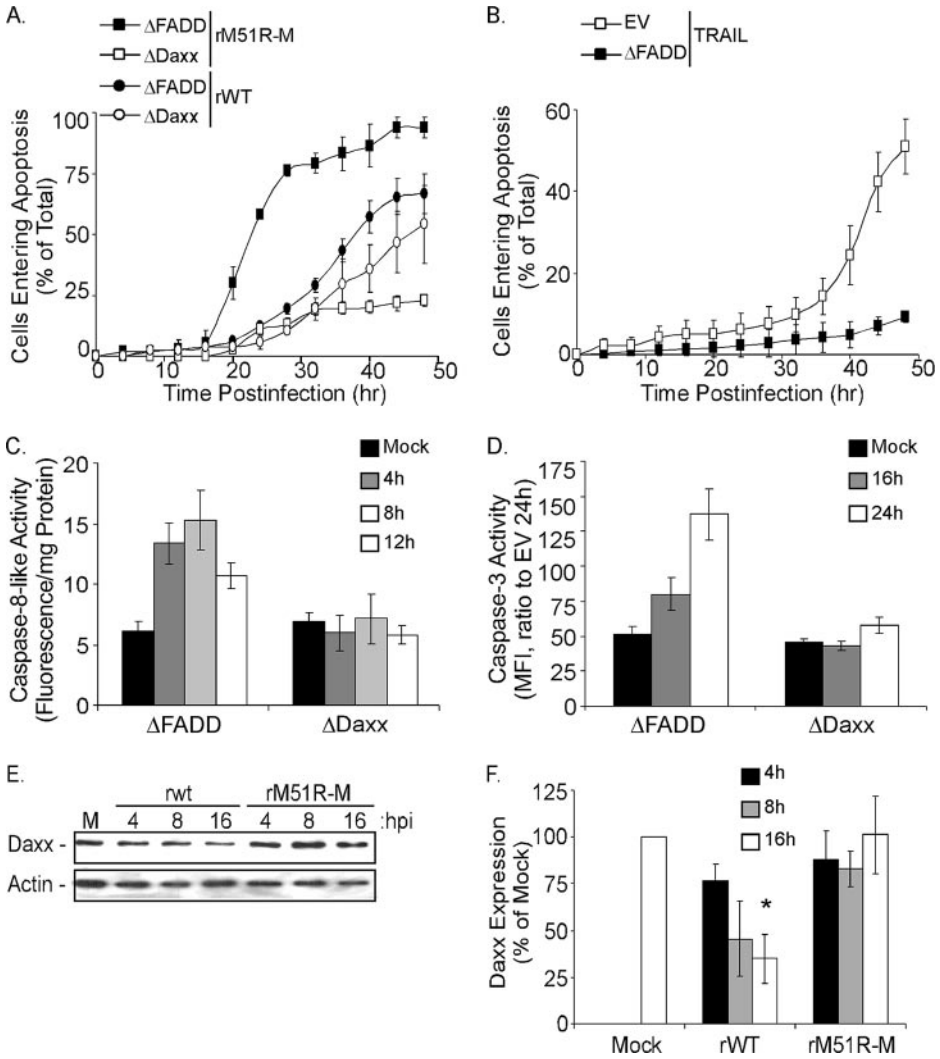

FIG. 4. Daxx is more important than FADD for apoptosis induced by rM51R-M virus. (A) L929 cells stably expressing dominant-negative mutants of FADD (ΔFADD) and Daxx (ΔDaxx) were infected with rM51R-M or rWT viruses. The cumulative percentage of cells entering apoptosis was determined using time-lapse video microscopy as described in the legend to Fig. 3. The data represent the averages ± SEM of three experiments. (B) L929-EV and L929-ΔFADD cells were treated with 50 nM TRAIL. Cells entering apoptosis were monitored using time-lapse video microscopy as described in the legend to Fig. 3. The data represent the averages ± SEM of three experiments. (C) Fluorometric caspase-8 assays were performed using L929-ΔFADD and L929-ΔDaxx cells that were mock infected or infected with rM51R-M virus. Cell lysates were obtained at the indicated times postinfection, and caspase-8 activity was measured using a fluorometric substrate. The data represent the averages ± SEM of three experiments. (D) Caspase-3 activity was measured via flow cytometry in mock-infected and rM51R-M virus-infected L929-ΔFADD and L929-ΔDaxx cells using PE-conjugated antibodies against active caspase-3. Data are expressed as the geometric mean fluorescence intensity (MFI) normalized to the maximum level observed in EV cells. The data represent the averages ± SEM of three experiments. (E) L929 cells were mock infected or infected with rWT or rM51R-M viruses. At the indicated times postinfection, cell lysates were analyzed via Western blotting with antibodies for Daxx and β-actin. (F) Western blots were quantitated via densitometric analysis. Levels of Daxx protein expression were normalized to levels of actin for each sample. Results indicate the averages of three independent experiments ± SEM ($*P < 0.05$ relative to mock-infected samples). hpi, hours postinfection.

(Fig. 3F). Taken together, the data presented in Fig. 3 indicate that Fas and PKR play important roles in apoptosis induced by rM51R-M virus, further supporting the model that induction of apoptosis by M protein mutant VSV is a result of the activation of host antiviral responses.

Daxx is more important than FADD for apoptotic signaling induced by rM51R-M virus. Two different adaptor molecules, FADD and Daxx, have been implicated in Fas signaling. The large increase in Daxx gene expression coupled with the suppression of FADD gene expression during rM51R-M virus infection (Fig. 1A) suggested that Daxx may play an important role in rM51R-M virus-induced apoptosis. Research from many laboratories has focused on FADD as a necessary transducer of Fas-mediated apoptosis (18, 63). In contrast, the role of Daxx in Fas-mediated apoptosis remains controversial (39, 47). To analyze the potential role of Daxx in VSV-induced apoptosis, we initially attempted to knock down Daxx expression using small interfering RNA. However, we were unable to detect changes in Daxx expression using any of several small interfering RNAs tested (data not shown). Therefore, to com-

pare the roles of Daxx and FADD in VSV-induced apoptosis, we generated L929 cells that stably express dominant-negative mutants of these proteins, L929-ΔDaxx and L929-ΔFADD, respectively. ΔFADD is a truncation mutant that consists solely of the FADD death domain. This mutant is capable of binding the death domain of Fas but is unable to recruit and activate caspase-8 (48). ΔDaxx is a truncation mutant composed of the C-terminal 114 amino acids that bind to the Fas death domain. Like ΔFADD, this mutant is able to bind the Fas death domain but is unable to recruit downstream effector molecules to initiate a proapoptotic cascade (54, 71).

L929-ΔFADD or L929-ΔDaxx cells were infected with rWT virus or rM51R-M virus, and cells entering apoptosis were quantitated using time-lapse microscopy (Fig. 4A). Both rWT and rM51R-M viruses induced apoptosis in L929-ΔFADD cells at rates similar to those for L929-EV cells (shown in Fig. 3A and B), suggesting that FADD has little if any role in rM51R-M or rWT virus-induced apoptosis (Fig. 4A). In contrast to ΔFADD, the expression of ΔDaxx almost completely abolished apoptosis induced by rM51R-M virus, while the rate of apoptosis induced by rWT virus in L929-ΔDaxx cells was almost indistinguishable from that seen in L929-ΔFADD cells (Fig. 4A). These data suggest that, unlike FADD, Daxx plays a prominent role in Fas-mediated apoptosis in response to infection with rM51R-M virus but not rWT virus.

In order to interpret the inability of ΔFADD to inhibit the induction of apoptosis, it was important to have a positive control for the effects of ΔFADD. L929-EV and L929-ΔFADD cells were treated with TRAIL, which is known to induce apoptosis through FADD-dependent signaling. Treatment with TRAIL induced apoptosis in L929-EV cells, but TRAIL-induced apoptosis was completely inhibited in cells expressing ΔFADD (Fig. 4B), verifying that ΔFADD exhibits dominant-negative activity.

To confirm the rate of apoptosis determined by time-lapse microscopy, caspase-8-like activity and levels of active caspase-3 were analyzed as a function of time in L929-ΔFADD and L929-ΔDaxx cells (Fig. 4C and D). The maximum level of caspase-8-like activity was observed in L929-ΔFADD cells at 8 h postinfection with rM51R-M virus, similar to the results with L929-EV cells (Fig. 3C). However, caspase-8-like activity in L929-ΔDaxx remained at background levels throughout this time course (Fig. 4C). Similarly, high levels of active caspase-3 were detected at 24 h postinfection with rM51R-M virus in L929-ΔFADD cells, while rM51R-M virus failed to activate caspase-3 in L929-ΔDaxx cells (Fig. 4D). These data further support the idea that Fas-mediated activation of caspases in response to rM51R-M virus infection is dependent on Daxx signaling but not FADD signaling.

The results of the microarray analysis (Fig. 1) indicated that Daxx mRNA expression is upregulated in response to rM51R-M virus infection. To determine the levels of Daxx protein expression, Western blot analysis was carried out using mock- and VSV-infected L929 cells. As seen in Fig. 4E and F, Daxx protein expression decreased significantly by 16 h postinfection with rWT virus. However, Daxx protein was maintained at high levels in rM51R-M virus-infected cells, suggesting that the new mRNA expression induced by rM51R-M virus infection serves to replenish Daxx in L929 cells faster than it can be degraded. Taken together, the data presented in Fig. 4 indicate that Daxx is more

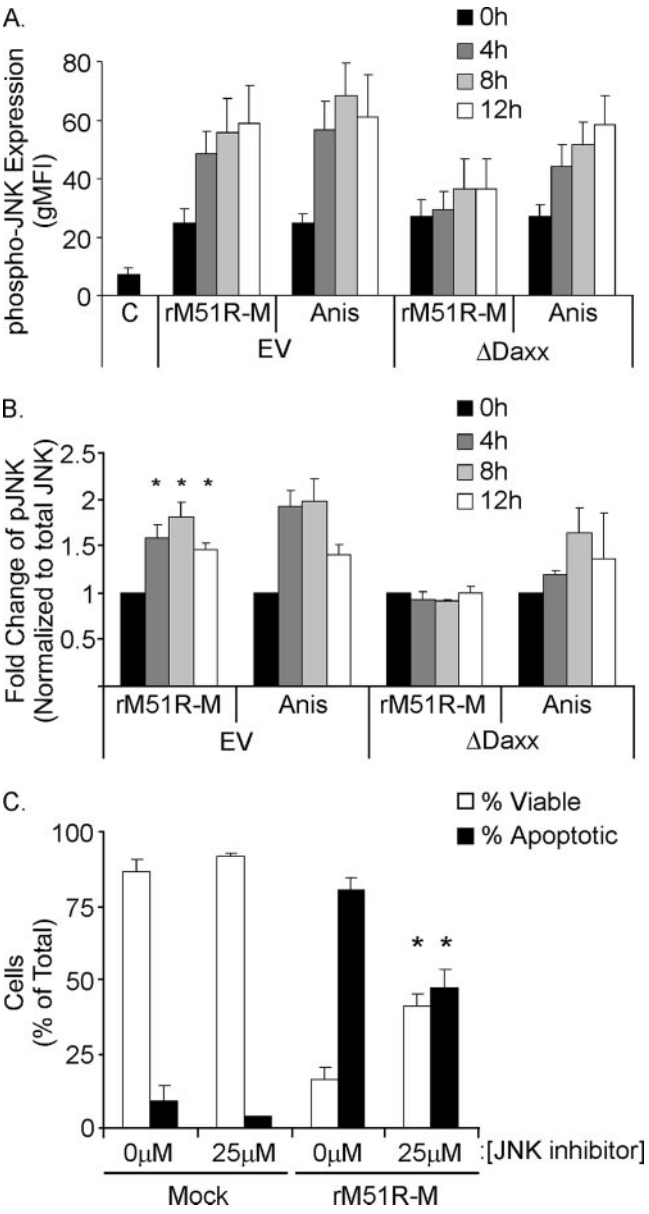

FIG. 5. JNK activation is required for Daxx-mediated apoptosis. (A) JNK activation was monitored in L929-EV and L929-ΔDaxx cells by measuring the levels of phosphorylated JNK at the indicated times postinfection with rM51R-M virus or posttreatment with anisomycin. Phosphorylated JNK was detected via flow cytometry using antibodies specific for JNK phosphorylated at Thr183 and Tyr185. Data are expressed as the geometric mean fluorescence intensity (gMFI) compared to cells labeled with total rabbit serum as a primary antibody control (C). (B) Levels of phosphorylated JNK determined in A were normalized to levels of total JNK. Results are shown as the change (*n*-fold) in phosphorylated JNK in rM51R-M virus-infected cells and anisomycin-treated cells above the background observed in untreated cells. (C) Apoptosis in the presence and absence of a specific inhibitor of JNK activity (SP600125; 25 μM) was measured via flow cytometry by staining with annexin V and 7-AAD. Data are presented as percentages of viable cells (annexin V negative) and apoptotic cells (annexin V positive) and represent the averages ± SEM of three experiments ($*P < 0.05$ relative to samples not treated with JNK inhibitor).

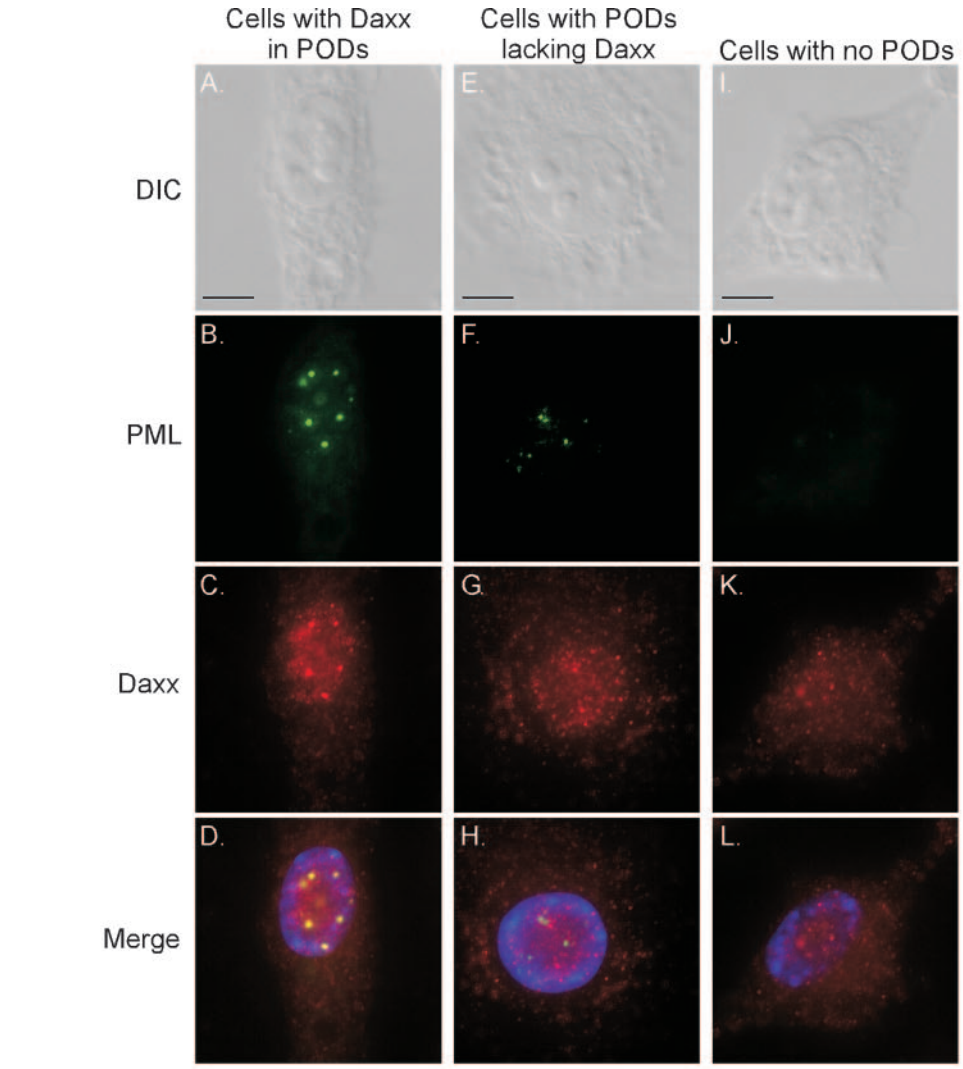

M.

Cells	hpi	% Cells w/ Daxx in PODs	% Cells w/ PODs lacking Daxx	% Cells w/ no PODs
EV	0	85.0 ± 3.4	12.0 ± 3.0	3.0 ± 1.8
EV	16	52.9 ± 12.9	32.5 ± 7.0	14.5 ± 5.9
ΔDaxx	0	79.3 ± 9.0	15.8 ± 11.0	4.9 ± 3.5
ΔDaxx	16	56.0 ± 9.8	20.2 ± 9.4	23.8 ± 8.3

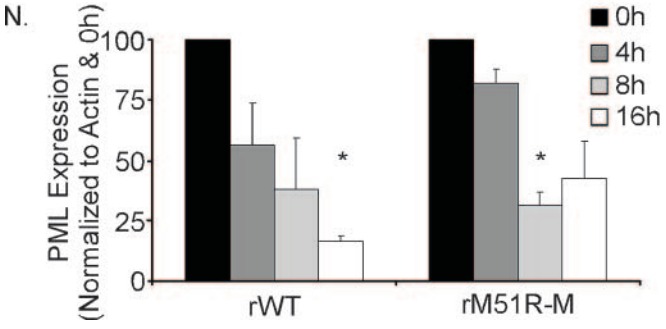

FIG. 6. Daxx localization to PODs changes in response to rM51R-M virus infection. L929-EV and L929-ΔDaxx cells were mock infected or infected with rM51R-M virus. At 16 h postinfection (hpi), cells were analyzed by indirect immunofluorescence as described in Materials and

important than FADD in the induction of apoptosis in response to rM51R-M virus infection.

Daxx-mediated apoptosis is dependent on signaling through JNK. Upon binding to the Fas death domain, Daxx has been shown to recruit and activate apoptosis signal-regulating kinase 1 (ASK1), which subsequently activates JNK (14, 71). Therefore, the activation of JNK was examined to obtain further evidence that Daxx was activated in response to rM51R-M virus infection and to begin to elucidate the mechanism by which Daxx contributes to apoptosis induction. The activation of JNK involves phosphorylation by various upstream protein kinases. Antibodies specific for phosphorylated versus total JNK were used to measure JNK activation using flow cytometry (Fig. 5A and B). In untreated cells, JNK was phosphorylated at low levels, corresponding to an approximately 2.5-fold increase in fluorescence above a nonspecific antibody control. Treatment with anisomycin served as the positive control for JNK activation. At 4 h and 8 h posttreatment of L929-EV cells with anisomycin, levels of phosphorylated JNK increased dramatically above levels seen in untreated cells. Following infection with rM51R-M virus, JNK was phosphorylated to levels similar to those seen following treatment with anisomycin (Fig. 5A). The expression of ΔDaxx did not prevent the increased phosphorylation of JNK in response to anisomycin treatment. However, ΔDaxx inhibited the increased phosphorylation of JNK in response to rM51R-M virus infection (Fig. 5A). Levels of phosphorylated JNK were normalized to the levels of total JNK as determined by flow cytometry with an antibody against total JNK. This ratio is expressed in Fig. 5B as the change (*n*-fold) above mock-infected cells. Treatment with anisomycin or infection with rM51R-M virus increased JNK activation to levels that were approximately twofold higher than the levels in untreated L929-EV cells. The expression of ΔDaxx prevented the activation of JNK by rM51R-M virus, confirming that JNK was activated downstream of Daxx in rM51R-M virus-induced apoptosis (Fig. 5B).

To determine if JNK is involved in Daxx-dependent apoptosis in response to rM51R-M virus infection, apoptosis was measured at 24 h postinfection in the presence or absence of a synthetic JNK inhibitor (SP600125; 25 μM). Apoptosis was measured by fluorescent labeling with annexin V and 7-AAD. As shown in Fig. 5B, infection with rM51R-M virus in the absence of the JNK inhibitor resulted in extensive apoptosis. On the other hand, treatment with the JNK inhibitor significantly reduced the percentage of apoptotic cells while significantly increasing the percentage of viable cells (Fig. 5B). These data further support the idea that JNK plays an important role in rM51R-M virus-induced apoptosis.

Daxx is present in both the nucleus and cytoplasm of rM51R-M virus-infected cells. The role of Daxx in apoptosis, particularly Fas-mediated apoptosis, remains a controversial issue (39, 47). The originally identified cytoplasmic functions of Daxx, such as acting as an adaptor protein for Fas, have been challenged by reports that Daxx is present exclusively in the nucleus, specifically localized in PML oncogenic domains (PODs), and that Daxx exerts its proapoptotic effects by acting as a transcription regulator (37, 55, 75). To address the issue of Daxx localization in the case of rM51R-M virus infection, immunofluorescence microscopy was used to determine the localization of Daxx and PML at various times postinfection in L929-EV cells and L929-ΔDaxx cells. Figure 6 (A to L) shows examples of the three different labeling patterns for Daxx and PML observed in these experiments, and Fig. 6M shows the percentage of total cells with each pattern. In a majority of cells, Daxx appeared in a speckled pattern throughout the nucleus and cytoplasm, with the nucleus appearing to be somewhat more brightly labeled than the cytoplasm (Fig. 6C, G, and K). It was determined that nuclear Daxx labeling was approximately four times brighter than cytoplasmic Daxx, suggesting that Daxx was present in much higher quantities in the nucleus than in the cytoplasm (data not shown). The speckled pattern of Daxx labeling in the nucleus colocalized with PML (Fig. 6B, C, and D). A similar pattern of Daxx labeling was observed in both L929-EV and L929-ΔDaxx cells, suggesting that the expression of ΔDaxx does not interfere with localization to the nucleus or cytoplasm.

Following infection with rM51R-M virus, two distinct changes in PML labeling were observed. First, in many cells, Daxx was maintained in its speckled pattern of labeling throughout the nucleus and cytoplasm, but its localization did not correspond to that of PML (Fig. 6E to H). Second, the number of cells lacking POD structures increased following infection with rM51R-M virus (Fig. 6I to L shows an example). Similar results were obtained in both L929-EV cells and L929-ΔDaxx cells (Fig. 6M). The disappearance of PML from infected cells corresponded to a statistically significant decrease in total levels of PML as determined by Western blot analysis (Fig. 6N). These data provide evidence that the subcellular localization of Daxx is consistent with all of the functions that have been postulated for Daxx in the induction of apoptosis: as a cytoplasmic factor able to interact with the Fas death receptor and as a nuclear factor involved in the regulation of apoptosis-related genes.

DISCUSSION

We have previously demonstrated that apoptosis induced by rM51R-M virus requires new host gene expression and activation of the extrinsic apoptotic pathway (29). These observations led to the hypothesis that rM51R-M virus-induced apoptosis occurs due to host antiviral responses. Virus-induced

Methods using antibodies specific for PML and Daxx. Bar, 10 μm. (A to L) Representative cells that illustrate the three patterns of Daxx and PML labeling observed: cells expressing Daxx in PODs, cells expressing PODs without Daxx, and cells not expressing PODs. (M) Quantification of cells expressing Daxx in PODs, cells expressing PODs without Daxx, and cells not expressing PODs. Data are expressed as percentages of total cells ± SEM for three experiments. (N) Cells were mock infected or infected with rWT virus or rM51R-M virus. At the indicated times postinfection, cell lysates were analyzed via Western blotting with antibodies for PML and β-actin. Western blots were quantitated via densitometric analysis. Levels of PML protein expression were normalized to levels of actin for each sample. Results indicate the averages of three independent experiments ± SEM ($*P < 0.05$ relative to mock-infected samples). DIC, differential interference contrast.

apoptosis that is mediated by host antiviral responses has been shown to involve upstream mediators such as Fas and PKR (6, 8, 28, 60). Here, we demonstrate that apoptosis induction by rM51R-M virus involves the Fas death receptor pathway as well as PKR (Fig. 3). Surprisingly, the expression of a dominant-negative form of FADD did not inhibit rM51R-M virus-induced apoptosis (Fig. 4). Instead, the activation of apoptosis by rM51R-M virus was more sensitive to the inhibition of Daxx, an alternative Fas adaptor protein (Fig. 4). These results support the idea that Daxx is more important than FADD for rM51R-M virus-induced apoptosis. While Daxx has previously been implicated in antiviral responses against a variety of viruses (13, 33, 44, 62, 74), to our knowledge, this is the first report of a requirement for Daxx in virus-induced apoptosis. Furthermore, our work suggests a new pathway for Fas-mediated apoptosis in which Daxx can take the place of FADD in transducing Fas death signals.

Evidence that rM51R-M virus activates the Fas pathway includes the translocation of Fas to the cell surface from intracellular stores (Fig. 2B and C) and the inhibition of apoptosis by the dominant-negative Fas mutant (Fig. 3). The activation of the Fas death receptor pathway may occur extracellularly via the ligation of Fas by Fas ligand (FasL) or intracellularly due to signaling through other pathways (6, 31, 63). Our attempts to demonstrate a role for FasL gave largely negative results (Fig. 2E). This raised the possibility that the Fas pathway was not activated by FasL extracellularly in response to rM51R-M virus infection. Similar activation of Fas without evidence of FasL involvement has been observed in cells responding to other stimuli, such as reactive nitrogen species, UVA irradiation, and ether lipid treatment (30, 57, 76).

The inhibition of PKR by 2-AP or the expression of ΔPKR prevented apoptosis induced by rM51R-M virus (Fig. 3), suggesting that PKR plays an important role in activating the Fas pathway in response to this virus. While previous reports that PKR activates the Fas pathway suggested that this mechanism of apoptosis is FADD dependent, we propose that PKR may also have a role in regulating Daxx signaling. In support of this, PKR has been shown to have a role in the modulation of ASK1, a protein kinase that interacts with Daxx and is important for the activation of JNK during Fas-mediated apoptosis (14, 61).

Despite nearly a decade of study, the role of Daxx in apoptosis remains a controversial issue. What is clear is that Daxx has multiple functions and that some of these functions lead to apoptosis (32, 39, 40, 47, 54, 65, 71, 75). Daxx was originally identified as a Fas death domain-binding protein that enhanced Fas-mediated apoptosis by binding ASK1 and activating downstream mitogen-activated protein kinase, specifically JNK (14, 71). It has also been suggested that Daxx binds transforming growth factor β receptor II and sensitizes cells to transforming growth factor β-induced apoptosis (53). According to these models, Daxx is likely part of the death-inducing signaling complex, allowing a direct interaction with death receptors. Daxx then signals through stress kinases, such as JNK, and unidentified downstream mediators to activate caspases, leading to apoptosis. However, it has been difficult to demonstrate that Daxx is a component of the death-inducing signaling complex, and evidence for functions of Daxx that are independent of Fas raises the possibility of an alternative model. For example, some groups previously reported that Daxx is present exclusively in the nucleus, where it elicits its proapoptotic effect by acting as a transcriptional regulator (32, 37, 65, 75). Furthermore, it is well documented that Daxx interacts with nuclear bodies or PODs (37, 65). However, it is not known whether the localization of Daxx to PODs is required for its proapoptotic effect or if PODs serve as storage sites to sequester Daxx away from its targets (43, 75). We show that Daxx was found in both the nucleus and the cytoplasm and that in uninfected cells, Daxx colocalized with PML in PODs. However, by 16 h postinfection, a significant percentage of PODs were disrupted, as shown by cells with smaller PODs that no longer contained Daxx or by cells that no longer expressed detectable levels of PML (Fig. 6). These data suggest that VSV infection may result not only in the disruption of PODs but perhaps also in the degradation of PML. While several DNA viruses have been shown to interact with and even disrupt PODs (21, 26, 36, 70), such functions have never been reported for VSV. On the other hand, PML has been suggested to contribute to the antiviral response against RNA viruses, including VSV and influenza virus, independent of its localization to PODs (15). Similarly, our data support a model in which Daxx associated with PODs in uninfected cells may be released to participate in the induction of apoptosis following virus infection.

These results have important implications for oncolytic VSV therapy as well as cancer therapy in general. The data presented here suggest that oncolytic M protein mutants of VSV may be particularly effective against tumors that upregulate Daxx mRNA in response to virus infection. Furthermore, some cancers have been shown to downregulate FADD during the process of tumorigenesis, allowing these tumors to become resistant to the extrinsic apoptotic pathway (64). Our results demonstrate that rM51R-M virus activates the extrinsic pathway when FADD signaling is inhibited, suggesting that this virus may be particularly useful in treating tumors that have downregulated FADD. In addition, the observation that rM51R-M virus activates the Fas death receptor pathway presents the potential for various mechanisms to enhance cell death induced by this virus. VSV is easily manipulated genetically, offering the possibility of expressing transgenes from the virus genome that may enhance the activation of the Fas pathway. Similarly, this presents the possibility of combinatorial therapies with chemotherapeutic drugs that target the extrinsic pathway or the intrinsic pathway, which would allow the activation of both of the major apoptotic pathways. Finally, these results suggest a novel Fas-mediated apoptotic pathway that utilizes Daxx instead of FADD, presenting a promising new target for rational therapeutic strategies.

ACKNOWLEDGMENTS

We acknowledge the Microscopy Core Laboratory at Wake Forest University. We thank Maryam Ahmed and John Connor for helpful advice and comments on the manuscript. We also thank Randall Kaufman and Andrew Thorburn for sharing plasmid DNAs and Sharmila Pejawar for assistance with flow cytometry experiments.

This work was supported by Public Health Service grant AI 32983 from the National Institute of Allergy and Infectious Diseases. The Microscopy Core Laboratory was supported in part by a core grant

for the Comprehensive Cancer Center of Wake Forest University, CA12197, from the National Cancer Institute.

REFERENCES

1. **Ahmed, M., S. D. Cramer, and D. S. Lyles.** 2004. Sensitivity of prostate tumors to wild type and M protein mutant vesicular stomatitis viruses. Virology **330:**34–49.
2. **Ahmed, M., M. O. McKenzie, S. Puckett, M. Hojnacki, L. Poliquin, and D. S. Lyles.** 2003. Ability of the matrix protein of vesicular stomatitis virus to suppress beta interferon gene expression is genetically correlated with the inhibition of host RNA and protein synthesis. J. Virol. **77:**4646–4657.
3. **Augstein, P., A. Dunger, C. Salzsieder, P. Heinke, R. Kubernath, J. Bahr, U. Fischer, R. Rettig, and E. Salzsieder.** 2002. Cell surface trafficking of Fas in NIT-1 cells and dissection of surface and total Fas expression. Biochem. Biophys. Res. Commun. **290:**443–451.
4. **Balachandran, S., and G. N. Barber.** 2004. Defective translational control facilitates vesicular stomatitis virus oncolysis. Cancer Cell **5:**51–65.
5. **Balachandran, S., and G. N. Barber.** 2000. Vesicular stomatitis virus (VSV) therapy of tumors. IUBMB Life **50:**135–138.
6. **Balachandran, S., C. N. Kim, W. C. Yeh, T. W. Mak, K. Bhalla, and G. N. Barber.** 1998. Activation of the dsRNA-dependent protein kinase, PKR, induces apoptosis through FADD-mediated death signaling. EMBO J. **17:** 6888–6902.
7. **Balachandran, S., M. Porosnicu, and G. N. Barber.** 2001. Oncolytic activity of vesicular stomatitis virus is effective against tumors exhibiting aberrant p53, Ras, or Myc function and involves the induction of apoptosis. J. Virol. **75:**3474–3479.
8. **Balachandran, S., P. C. Roberts, T. Kipperman, K. N. Bhalla, R. W. Compans, D. R. Archer, and G. N. Barber.** 2000. Alpha/beta interferons potentiate virus-induced apoptosis through activation of the FADD/caspase-8 death signaling pathway. J. Virol. **74:**1513–1523.
9. **Bell, J. C., B. Lichty, and D. Stojdl.** 2003. Getting oncolytic virus therapies off the ground. Cancer Cell **4:**7–11.
10. **Benedict, C. A., T. A. Banks, and C. F. Ware.** 2003. Death and survival: viral regulation of TNF signaling pathways. Curr. Opin. Immunol. **15:**59–65.
11. **Black, B. L., R. B. Rhodes, M. McKenzie, and D. S. Lyles.** 1993. The role of vesicular stomatitis virus matrix protein in inhibition of host-directed gene expression is genetically separable from its function in virus assembly. J. Virol. **67:**4814–4821.
12. **Boehrer, S., D. Nowak, S. Hochmuth, S. Z. Kim, B. Trepohl, A. Afkir, D. Hoelzer, P. S. Mitrou, E. Weidmann, and K. U. Chow.** 2005. Daxx overexpression in T-lymphoblastic Jurkat cells enhances caspase-dependent death receptor- and drug-induced apoptosis in distinct ways. Cell. Signal. **17:**581–595.
13. **Cantrell, S. R., and W. A. Bresnahan.** 2005. Interaction between the human cytomegalovirus UL82 gene product (pp71) and hDaxx regulates immediate-early gene expression and viral replication. J. Virol. **79:**7792–7802.
14. **Chang, H. Y., H. Nishitoh, X. Yang, H. Ichijo, and D. Baltimore.** 1998. Activation of apoptosis signal-regulating kinase 1 (ASK1) by the adapter protein Daxx. Science **281:**1860–1863.
15. **Chelbi-Alix, M. K., F. Quignon, L. Pelicano, M. H. Koken, and H. de The.** 1998. Resistance to virus infection conferred by the interferon-induced promyelocytic leukemia protein. J. Virol. **72:**1043–1051.
16. **Clarke, P., and K. L. Tyler.** 2003. Reovirus-induced apoptosis: a minireview. Apoptosis **8:**141–150.
17. **Connor, J. H., C. Naczki, C. Koumenis, and D. S. Lyles.** 2004. Replication and cytopathic effect of oncolytic vesicular stomatitis virus in hypoxic tumor cells in vitro and in vivo. J. Virol. **78:**8960–8970.
18. **Curtin, J. F., and T. G. Cotter.** 2003. Live and let die: regulatory mechanisms in Fas-mediated apoptosis. Cell. Signal. **15:**983–992.
19. **Der, S. D., Y. L. Yang, C. Weissmann, and B. R. Williams.** 1997. A double-stranded RNA-activated protein kinase-dependent pathway mediating stress-induced apoptosis. Proc. Natl. Acad. Sci. USA **94:**3279–3283.
20. **Donze, O., J. Dostie, and N. Sonenberg.** 1999. Regulatable expression of the interferon-induced double-stranded RNA dependent protein kinase PKR induces apoptosis and fas receptor expression. Virology **256:**322–329.
21. **Doucas, V., A. M. Ishov, A. Romo, H. Juguilon, M. D. Weitzman, R. M. Evans, and G. G. Maul.** 1996. Adenovirus replication is coupled with the dynamic properties of the PML nuclear structure. Genes Dev. **10:**196–207.
22. **Ebert, O., S. Harbaran, K. Shinozaki, and S. L. Woo.** 2005. Systemic therapy of experimental breast cancer metastases by mutant vesicular stomatitis virus in immune-competent mice. Cancer Gene Ther. **12:**350–358.
23. **Ebert, O., K. Shinozaki, T. G. Huang, M. J. Savontaus, A. Garcia-Sastre, and S. L. Woo.** 2003. Oncolytic vesicular stomatitis virus for treatment of orthotopic hepatocellular carcinoma in immune-competent rats. Cancer Res. **63:**3605–3611.
24. **Ebert, O., K. Shinozaki, C. Kournioti, M. S. Park, A. Garcia-Sastre, and S. L. Woo.** 2004. Syncytia induction enhances the oncolytic potential of vesicular stomatitis virus in virotherapy for cancer. Cancer Res. **64:**3265–3270.
25. **Einhorn, S., and H. Strander.** 1993. Interferon treatment of human malignancies—a short review. Med. Oncol. Tumor Pharmacother. **10:**25–29.
26. **Everett, R. D., and G. G. Maul.** 1994. HSV-1 IE protein Vmw110 causes redistribution of PML. EMBO J. **13:**5062–5069.
27. **Fernandez, M., M. Porosnicu, D. Markovic, and G. N. Barber.** 2002. Genetically engineered vesicular stomatitis virus in gene therapy: application for treatment of malignant disease. J. Virol. **76:**895–904.
28. **Fujimoto, I., T. Takizawa, Y. Ohba, and Y. Nakanishi.** 1998. Co-expression of Fas and Fas-ligand on the surface of influenza virus-infected cells. Cell Death Differ. **5:**426–431.
29. **Gaddy, D. F., and D. S. Lyles.** 2005. Vesicular stomatitis viruses expressing wild-type or mutant M proteins activate apoptosis through distinct pathways. J. Virol. **79:**4170–4179.
30. **Gajate, C., R. I. Fonteriz, C. Cabaner, G. Alvarez-Noves, Y. Alvarez-Rodriguez, M. Modolell, and F. Mollinedo.** 2000. Intracellular triggering of Fas, independently of FasL, as a new mechanism of antitumor ether lipid-induced apoptosis. Int. J. Cancer **85:**674–682.
31. **Gil, J., and M. Esteban.** 2000. The interferon-induced protein kinase (PKR), triggers apoptosis through FADD-mediated activation of caspase 8 in a manner independent of Fas and TNF-alpha receptors. Oncogene **19:**3665–3674.
32. **Gostissa, M., M. Morelli, F. Mantovani, E. Guida, S. Piazza, L. Collavin, C. Brancolini, C. Schneider, and G. Del Sal.** 2004. The transcriptional repressor hDaxx potentiates p53-dependent apoptosis. J. Biol. Chem. **279:**48013–48023.
33. **Greger, J. G., R. A. Katz, A. M. Ishov, G. G. Maul, and A. M. Skalka.** 2005. The cellular protein Daxx interacts with avian sarcoma virus integrase and viral DNA to repress viral transcription. J. Virol. **79:**4610–4618.
34. **Hofmann, H., H. Sindre, and T. Stamminger.** 2002. Functional interaction between the pp71 protein of human cytomegalovirus and the PML-interacting protein human Daxx. J. Virol. **76:**5769–5783.
35. **Huang, T. G., O. Ebert, K. Shinozaki, A. Garcia-Sastre, and S. L. Woo.** 2003. Oncolysis of hepatic metastasis of colorectal cancer by recombinant vesicular stomatitis virus in immune-competent mice. Mol. Ther. **8:**434–440.
36. **Ishov, A. M., and G. G. Maul.** 1996. The periphery of nuclear domain 10 (ND10) as site of DNA virus deposition. J. Cell Biol. **134:**815–826.
37. **Ishov, A. M., A. G. Sotnikov, D. Negorev, O. V. Vladimirova, N. Neff, T. Kamitani, E. T. Yeh, J. F. Strauss III, and G. G. Maul.** 1999. PML is critical for ND10 formation and recruits the PML-interacting protein daxx to this nuclear structure when modified by SUMO-1. J. Cell Biol. **147:**221–234.
38. **Kayagaki, N., A. Kawasaki, T. Ebata, H. Ohmoto, S. Ikeda, S. Inoue, K. Yoshino, K. Okumura, and H. Yagita.** 1995. Metalloproteinase-mediated release of human Fas ligand. J. Exp. Med. **182:**1777–1783.
39. **Khelifi, A. F., M. S. D'Alcontres, and P. Salomoni.** 2005. Daxx is required for stress-induced cell death and JNK activation. Cell Death Differ. **12:**724–733.
40. **Ko, Y. G., Y. S. Kang, H. Park, W. Seol, J. Kim, T. Kim, H. S. Park, E. J. Choi, and S. Kim.** 2001. Apoptosis signal-regulating kinase 1 controls the proapoptotic function of death-associated protein (Daxx) in the cytoplasm. J. Biol. Chem. **276:**39103–39106.
41. **Kopecky, S. A., and D. S. Lyles.** 2003. Contrasting effects of matrix protein on apoptosis in HeLa and BHK cells infected with vesicular stomatitis virus are due to inhibition of host gene expression. J. Virol. **77:**4658–4669.
42. **Kopecky, S. A., M. C. Willingham, and D. S. Lyles.** 2001. Matrix protein and another viral component contribute to induction of apoptosis in cells infected with vesicular stomatitis virus. J. Virol. **75:**12169–12181.
43. **Li, H., C. Leo, J. Zhu, X. Wu, J. O'Neil, E. J. Park, and J. D. Chen.** 2000. Sequestration and inhibition of Daxx-mediated transcriptional repression by PML. Mol. Cell. Biol. **20:**1784–1796.
44. **Li, X. D., T. P. Makela, D. Guo, R. Soliymani, V. Koistinen, O. Vapalahti, A. Vaheri, and H. Lankinen.** 2002. Hantavirus nucleocapsid protein interacts with the Fas-mediated apoptosis enhancer Daxx. J. Gen. Virol. **83:**759–766.
45. **Lichty, B. D., D. F. Stojdl, R. A. Taylor, L. Miller, I. Frenkel, H. Atkins, and J. C. Bell.** 2004. Vesicular stomatitis virus: a potential therapeutic virus for the treatment of hematologic malignancy. Hum. Gene Ther. **15:**821–831.
46. **Lyles, D. S.** 2000. Cytopathogenesis and inhibition of host gene expression by RNA viruses. Microbiol. Mol. Biol. Rev. **64:**709–724.
47. **Michaelson, J. S.** 2000. The Daxx enigma. Apoptosis **5:**217–220.
48. **Morgan, M. J., J. Thorburn, L. Thomas, T. Maxwell, A. R. Brothman, and A. Thorburn.** 2001. An apoptosis signaling pathway induced by the death domain of FADD selectively kills normal but not cancerous prostate epithelial cells. Cell Death Differ. **8:**696–705.
49. **Muller, U., U. Steinhoff, L. F. Reis, S. Hemmi, J. Pavlovic, R. M. Zinkernagel, and M. Aguet.** 1994. Functional role of type I and type II interferons in antiviral defense. Science **264:**1918–1921.
50. **Nava, V. E., A. Rosen, M. A. Veliuona, R. J. Clem, B. Levine, and J. M. Hardwick.** 1998. Sindbis virus induces apoptosis through a caspase-dependent, CrmA-sensitive pathway. J. Virol. **72:**452–459.
51. **Obuchi, M., M. Fernandez, and G. N. Barber.** 2003. Development of recombinant vesicular stomatitis viruses that exploit defects in host defense to augment specific oncolytic activity. J. Virol. **77:**8843–8856.
52. **Ornelles, D. A., and T. Shenk.** 1991. Localization of the adenovirus early region 1B 55-kilodalton protein during lytic infection: association with nuclear viral inclusions requires the early region 4 34-kilodalton protein. J. Virol. **65:**424–429.
53. **Perlman, R., W. P. Schiemann, M. W. Brooks, H. F. Lodish, and R. A.**

Weinberg. 2001. TGF-beta-induced apoptosis is mediated by the adapter protein Daxx that facilitates JNK activation. Nat. Cell Biol. **3:**708–714.

54. **Raoul, C., C. Barthelemy, A. Couzinet, D. Hancock, B. Pettmann, and A. O. Hueber.** 2005. Expression of a dominant negative form of Daxx in vivo rescues motoneurons from Fas (CD95)-induced cell death. J. Neurobiol. **62:**178–188.
55. **Salomoni, P., and P. P. Pandolfi.** 2002. The role of PML in tumor suppression. Cell **108:**165–170.
56. **Shinozaki, K., O. Ebert, A. Suriawinata, S. N. Thung, and S. L. Woo.** 2005. Prophylactic alpha interferon treatment increases the therapeutic index of oncolytic vesicular stomatitis virus virotherapy for advanced hepatocellular carcinoma in immune-competent rats. J. Virol. **79:**13705–13713.
57. **Shrivastava, P., C. Pantano, R. Watkin, B. McElhinney, A. Guala, M. L. Poynter, R. L. Persinger, R. Budd, and Y. Janssen-Heininger.** 2004. Reactive nitrogen species-induced cell death requires Fas-dependent activation of c-Jun N-terminal kinase. Mol. Cell. Biol. **24:**6763–6772.
58. **Stojdl, D. F., B. Lichty, S. Knowles, R. Marius, H. Atkins, N. Sonenberg, and J. C. Bell.** 2000. Exploiting tumor-specific defects in the interferon pathway with a previously unknown oncolytic virus. Nat. Med. **6:**821–825.
59. **Stojdl, D. F., B. D. Lichty, B. R. tenOever, J. M. Paterson, A. T. Power, S. Knowles, R. Marius, J. Reynard, L. Poliquin, H. Atkins, E. G. Brown, R. K. Durbin, J. E. Durbin, J. Hiscott, and J. C. Bell.** 2003. VSV strains with defects in their ability to shutdown innate immunity are potent systemic anti-cancer agents. Cancer Cell **4:**263–275.
60. **Takizawa, T., K. Ohashi, and Y. Nakanishi.** 1996. Possible involvement of double-stranded RNA-activated protein kinase in cell death by influenza virus infection. J. Virol. **70:**8128–8132.
61. **Takizawa, T., C. Tatematsu, and Y. Nakanishi.** 2002. Double-stranded RNA-activated protein kinase interacts with apoptosis signal-regulating kinase 1. Implications for apoptosis signaling pathways. Eur. J. Biochem. **269:**6126–6132.
62. **Tang, Q., and G. G. Maul.** 2003. Mouse cytomegalovirus immediate-early protein 1 binds with host cell repressors to relieve suppressive effects on viral transcription and replication during lytic infection. J. Virol. **77:**1357–1367.
63. **Thorburn, A.** 2004. Death receptor-induced cell killing. Cell. Signal. **16:**139–144.
64. **Thorburn, J., F. Moore, A. Rao, W. W. Barclay, L. R. Thomas, K. W. Grant, S. D. Cramer, and A. Thorburn.** 2005. Selective inactivation of a Fas-associated death domain protein (FADD)-dependent apoptosis and autophagy pathway in immortal epithelial cells. Mol. Biol. Cell **16:**1189–1199.
65. **Torii, S., D. A. Egan, R. A. Evans, and J. C. Reed.** 1999. Human Daxx regulates Fas-induced apoptosis from nuclear PML oncogenic domains (PODs). EMBO J. **18:**6037–6049.
66. **Williams, B. A., A. P. Makrigiannis, J. Blay, and D. W. Hoskin.** 1997. Treatment of the P815 murine mastocytoma with cisplatin or etoposide up-regulates cell-surface Fas (CD95) expression and increases sensitivity to anti-Fas antibody-mediated cytotoxicity and to lysis by anti-CD3-activated killer-T cells. Int. J. Cancer **73:**416–423.
67. **Wollmann, G., P. Tattersall, and A. N. van den Pol.** 2005. Targeting human glioblastoma cells: comparison of nine viruses with oncolytic potential. J. Virol. **79:**6005–6022.
68. **Wong, L. H., K. G. Krauer, I. Hatzinisiriou, M. J. Estcourt, P. Hersey, N. D. Tam, S. Edmondson, R. J. Devenish, and S. J. Ralph.** 1997. Interferon-resistant human melanoma cells are deficient in ISGF3 components, STAT1, STAT2, and p48-ISGF3gamma. J. Biol. Chem. **272:**28779–28785.
69. **Wu, S., and R. J. Kaufman.** 1996. Double-stranded (ds) RNA binding and not dimerization correlates with the activation of the dsRNA-dependent protein kinase (PKR). J. Biol. Chem. **271:**1756–1763.
70. **Xu, Y., J. H. Ahn, M. Cheng, C. M. apRhys, C. J. Chiou, J. Zong, M. J. Matunis, and G. S. Hayward.** 2001. Proteasome-independent disruption of PML oncogenic domains (PODs), but not covalent modification by SUMO-1, is required for human cytomegalovirus immediate-early protein IE1 to inhibit PML-mediated transcriptional repression. J. Virol. **75:**10683–10695.
71. **Yang, X., R. Khosravi-Far, H. Y. Chang, and D. Baltimore.** 1997. Daxx, a novel Fas-binding protein that activates JNK and apoptosis. Cell **89:**1067–1076.
72. **Yokota, A., E. Takeuchi, M. Iizuka, Y. Ikegami, H. Takayama, and N. Shinohara.** 2005. Prominent dominant negative effect of a mutant Fas molecule lacking death domain on cell-mediated induction of apoptosis. Mol. Immunol. **42:**71–78.
73. **Yonehara, S., A. Ishii, and M. Yonehara.** 1989. A cell-killing monoclonal antibody (anti-Fas) to a cell surface antigen co-downregulated with the receptor of tumor necrosis factor. J. Exp. Med. **169:**1747–1756.
74. **Zhao, L. Y., A. L. Colosimo, Y. Liu, Y. Wan, and D. Liao.** 2003. Adenovirus E1B 55-kilodalton oncoprotein binds to Daxx and eliminates enhancement of p53-dependent transcription by Daxx. J. Virol. **77:**11809–11821.
75. **Zhong, S., P. Salomoni, S. Ronchetti, A. Guo, D. Ruggero, and P. P. Pandolfi.** 2000. Promyelocytic leukemia protein (PML) and Daxx participate in a novel nuclear pathway for apoptosis. J. Exp. Med. **191:**631–640.
76. **Zhuang, S., and I. E. Kochevar.** 2003. Ultraviolet A radiation induces rapid apoptosis of human leukemia cells by Fas ligand-independent activation of the Fas death pathways. Photochem. Photobiol. **78:**61–67.